Available online at www.sciencedirect.com

SciVerse ScienceDirect

Mathematics and Computers in Simulation 99 (2014) 37–53

MATHEMATICS AND COMPUTERS IN SIMULATION

www.elsevier.com/locate/matcom

Original article

Approximation of the Fokker–Planck equation of the stochastic chemostat

Fabien Campillo [a,*], Marc Joannides [a,b], Irène Larramendy-Valverde [b]

[a] *MODEMIC Project-team, INRIA/INRA, UMR MISTEA, Montpellier, France*
[b] *Université Montpellier 2/I3M, Montpellier, France*

Received 23 November 2011; received in revised form 11 September 2012; accepted 3 April 2013
Available online 13 May 2013

Abstract

We consider a stochastic model of the two-dimensional chemostat as a diffusion process for the concentration of substrate and the concentration of biomass. The model allows for the washout phenomenon: the disappearance of the biomass inside the chemostat. We establish the Fokker–Planck equation associated with this diffusion process, in particular we describe the boundary conditions that modelize the washout. We propose an adapted finite difference scheme for the approximation of the solution of the Fokker–Planck equation.

Keywords: Chemostat; Stochastic differential equation; Fokker–Planck equation; Finite difference scheme

1. Introduction

Many biotechnological processes are modelized with the help of ordinary differential equations (ODE). For example, the dynamic for a single species/single substrate chemostat is classically modelized as [13]:

$$\dot{s}(t) = -k\,\mu(s(t))\,b(t) + D\,(s_{\text{in}} - s(t))\,, \tag{1a}$$

$$\dot{b}(t) = \{\mu(s(t)) - D\}\,b(t) \tag{1b}$$

where $b(t)$ and $s(t)$ are the concentrations of biomass and substrate at time t inside the chemostat. The parameters are the dilution rate D, the input substrate concentration s_{in}, and the stoichiometric coefficient k. The specific growth function $\mu(s)$ could be of the Monod (non-inhibitory) type:

$$\mu(s) = \frac{\mu_{\max}\, s}{k_s + s}\,, \tag{2}$$

where $\mu_{\max}$ is the maximum growth rate and k_s is the half-saturation; it could also be of the Haldane (inhibitory) type:

$$\mu(s) = \frac{\overline{\mu}\, s}{k_s + s + s^2/\alpha}\,. \tag{3}$$

* Corresponding author. Tel.: +33 683945763
E-mail address: Fabien.Campillo@inria.fr (F. Campillo).

0378-4754/$36.00
http://dx.doi.org/10.1016/j.matcom.2013.04.012

As pointed out in [2], the system (1) is simple and applicable to many situations, it can be seen as a limit model of a stochastic birth and death process in large population size asymptotic. Hence (1) can give account for the mean behavior of the underlying stochastic process but it cannot give account for its variance. Moreover (1) fails to propose a realistic representation of the chemostat in small population scenario, that is in cases close to the washout (corresponding to the disappearance of the biomass, i.e. $b(t)=0$) [3,4].

We present the stochastic model in Section 2 and derive the associated Fokker–Planck equation in Section 3. A finite difference scheme approximation is detailled in Section 4 and some numerical tests are presented in Section 5.

2. The stochastic chemostat model

Consider the stochastic process $X_t = (X_t^1, X_t^2) = (S_t, B_t)$ solution of:

$$\mathrm{d}S_t = \{-k\,\mu(S_t)\,B_t + D\,(s_{\mathrm{in}} - S_t)\}\,\mathrm{d}t + c_1\,\sqrt{S_t}\,\mathrm{d}W_t^1\,, \tag{4a}$$

$$\mathrm{d}B_t = \{\mu(S_t) - D\}\,B_t\,\mathrm{d}t + c_2\,\sqrt{B_t}\,\mathrm{d}W_t^2\,, \tag{4b}$$

where B_t and S_t are the concentrations of biomass and substrate at time t; W_t^1 and W_t^2 are independent scalar standard Brownian motions; $c_1>0$ and $c_2>0$ are the noise intensities; W_t^1 and W_t^2 are independent scalar standard Wiener processes [5]. We suppose that $S_0\geq 0$ and $B_0\geq 0$ so that $S_t\geq 0$ and $B_t\geq 0$ for all $t\geq 0$.

The process (4) is a diffusion approximation of a pure jump Markov process describing the dynamics of the chemostat at a microscopic level. The diffusion approximation approach leads to different stochastic models with the same drift coefficients but with different diffusion coefficients depending on the approximation assumptions adopted. In particular and in contrast with the case considered here, it is possible to obtain a system of SDEs with correlated Brownian motions [7]. The process (4) is in fact the simplest diffusion approximation. This diffusion approximation approach is detailed in [2], note that it ensures the non-negativeness of both components of (4).

The ordinary differential system (1) is an accurate representation of the pure jump process mentioned above in the case of infinite population size, while the stochastic differential system (4) is an accurate representation of this process in the case of large but finite population size. In other words, (1) is a representation of the pure jump process at a macroscopic scale as (4) is a representation at a mesoscopic scale.

Some highlights from the classic Cox-Ingersoll-Ross model will help us to describe the behavior of the solution of (4). Indeed, consider the one-dimensional SDE:

$$\mathrm{d}\xi_t = (a + b\,\xi_t)\;\mathrm{d}t + \sigma\,\sqrt{\xi_t}\;\mathrm{d}W_t\,,\quad \xi_0 = x_0 \geq 0\,. \tag{5}$$

with $a\geq 0$, $b\in\mathbb{R}$, $\sigma>0$. According to [11, Prop. 6.2.4], for all $x_0\geq 0$, ξ_t is a continuous process taking values in $\mathbb{R}^+$, and let $\tau = \inf\{t\geq 0,\ \xi_t = 0\}$, then:

(i) If $a\geq\sigma^2/2$, then $\tau=\infty$ $\mathbb{P}_x$–a.s.;
(ii) if $0\leq a<\sigma^2/2$ and $b\leq 0$ then $\tau<\infty$ $\mathbb{P}_x$–a.s.;
(iii) if $0\leq a<\sigma^2/2$ and $b>0$ then $\mathbb{P}_x(\tau<\infty)\in(0,1)$.

In the first case, ξ_t never reaches 0 almost surely. In the second case ξ_t a.s. reaches the state 0, in the third case it may reach 0. If $a=0$ then the state 0 is absorbing.

In case of the system (4), it is clear that $B=0$ is an absorbing state for (4b), and when $B=0$, (4a) reduces to the substrate dynamics conditionally on the washout, namely:

$$\mathrm{d}S_t^{\mathrm{w}} = D\,(s_{\mathrm{in}} - S_t^{\mathrm{w}})\,\mathrm{d}t + c_1\,\sqrt{S_t^{\mathrm{w}}}\,\mathrm{d}W_t^1 \tag{6}$$

hence the solution of this SDE will stay on the half-line
$[0,\infty)$ and:

1 if $D\,s_{\mathrm{in}}\geq\frac{c_1^2}{2}$ then S_t^{w} never reaches 0;
2 if $D\,s_{\mathrm{in}}<\frac{c_1^2}{2}$ then S_t^{w} reaches 0 in finite time and is reflected.

Note that, as c_1 is "small", condition (i) is more realistic than condition (ii): indeed, with a continuous input s_{in}, there is no reason for the substrate concentration in the chemostat to vanish.

Simulation schemes for (4) should respect the previous properties, a possible choice is (see [11] for other schemes):

$$S_{t+\delta} = [S_t + \{-k\,\mu(S_t)\,B_t + D\,(s_{\text{in}} - S_t)\}\,\delta + c_1\,\sqrt{S_t}\,\sqrt{\delta}\,w_t^1]_+\,, \tag{7a}$$

$$B_{t+\delta} = [B_t + \{\mu(S_t) - D\}\,B_t\,\delta + c_2\,\sqrt{B_t}\,\sqrt{\delta}\,w_t^2]_+\,, \tag{7b}$$

where $\{w_{i\delta}^1\}_{i\in\mathbb{N}}$ and $\{w_{i\delta}^2\}_{i\in\mathbb{N}}$ are i.i.d. $N(0,1)$ random variables, also independent from X_0. Note that $B_t = 0$ is absorbing for (7b).

Notations 2.1. Let $x = (x_1, x_2) = (s, b) \in \mathbb{R}_+^2 = [0,\infty)^2$ and

$$f_1(x) = f_1(s,b) \overset{\text{def}}{=} -k\,\mu(s)\,b + D\,(s_{\text{in}} - s)\,, \quad \sigma_1(x) = \sigma_1(s,b) = \sigma_1(s) \overset{\text{def}}{=} c_1\,\sqrt{s}\,,$$
$$f_2(x) = f_2(s,b) \overset{\text{def}}{=} [\mu(s) - D]\,b\,, \qquad\qquad \sigma_2(x) = \sigma_2(s,b) = \sigma_2(b) \overset{\text{def}}{=} c_2\,\sqrt{b}\,,$$

so that (4) reads:

$$\mathrm{d}X_t \;\; = f(X_t)\,\mathrm{d}t + \sigma(X_t)\,\mathrm{d}W_t$$

with $f(x) = \begin{pmatrix} f_1(x) \\ f_2(x) \end{pmatrix}$, $\sigma(x) = \begin{pmatrix} \sigma_1(x) & 0 \\ 0 & \sigma_2(x) \end{pmatrix}$ and $W_t = \begin{pmatrix} W_t^1 \\ W_t^2 \end{pmatrix}$.

Let $\partial\mathbb{R}_+^2 = \Gamma_1 \cup \Gamma_2$ with $\Gamma_1 = \{(s,b) \in [0,\infty)^2\,;\, b = 0\}$ and $\Gamma_2 = \{(s,b) \in [0,\infty)^2\,;\, s = 0\}$.

3. The Fokker–Planck equation

Let $\pi_t(\mathrm{d}x) = \pi_t(\mathrm{d}s, \mathrm{d}b)$ be the distribution law of of $X_t = (S_t, B_t)$:

$$\pi_t(A, B) = \mathbb{P}(S_t \in A\,, \quad B_t \in B)$$

for all Borel sets A, B of $[0,\infty)$. According to [12], $\pi_t(\mathrm{d}x)$ of X_t can be decomposed as:

$$\pi_t(\mathrm{d}x) = \pi_t(\mathrm{d}s \times \mathrm{d}b) = \delta_0(\mathrm{d}b)\,q_t(s)\,\mathrm{d}s + p_t(s,b)\,\mathrm{d}s\,\mathrm{d}b\,. \tag{8}$$

Indeed the diffusion process "lives" in $[0,\infty)^2$ but never reaches Γ_2 so that the distribution law features a "regular" component $p_t(s,b)$ which only charges $(0,\infty)^2$ and a "degenerate" component $q_t(s)$ which only charges Γ_1. The term $p_t(s,b)$ is the component corresponding to the non-washout and the term $q_t(s)$ is the component corresponding to the washout.

As π_t is a probability distribution we get the normalization property:

$$\int_0^\infty q_t(s)\,\mathrm{d}s + \int_0^\infty \int_0^\infty p_t(s,b)\,\mathrm{d}s\,\mathrm{d}b = 1$$

and the washout probability at time t is:

$$\mathbb{P}(B_t = 0) = \int_0^\infty q_t(s)\,\mathrm{d}s = 1 - \int_0^\infty \int_0^\infty p_t(s,b)\,\mathrm{d}s\,\mathrm{d}b\,.$$

The Fokker–Planck equation in a weak form is:

$$\frac{\mathrm{d}}{\mathrm{d}t}\iint_{\mathbb{R}_+^2} \pi_t(\mathrm{d}s, \mathrm{d}b)\,\phi(s,b) = \iint_{\mathbb{R}_+^2} \pi_t(\mathrm{d}s, \mathrm{d}b)\,\mathcal{L}\phi(s,b) \tag{9}$$

for all test functions ϕ, where $\mathcal{L}$ is the infinitesimal generator defined by:

$$\begin{aligned}\mathcal{L}\phi(x) &= \mathcal{L}\phi(s,b)\\ &\stackrel{\text{def}}{=} \sum_{i=1}^{2} f_i(x)\,\phi'_{x_i}(x) + \frac{1}{2}\sum_{i=1}^{2}\sigma_i^2(x)\,\phi''_{x_i^2}(x)\\ &= f_1(s,b)\,\phi'_s(s,b) + f_2(s,b)\,\phi'_b(s,b) + \frac{c_1^2}{2}\,s\,\phi''_{s^2}(s,b) + \frac{c_2^2}{2}\,b\,\phi''_{b^2}(s,b)\,.\end{aligned} \tag{10}$$

Using the decomposition (8), the Fokker–Planck equation (9) reads:

$$\begin{aligned}&\frac{\mathrm{d}}{\mathrm{d}t}\left\{\int_0^\infty q_t(s)\,\phi(s,0)\,\mathrm{d}s + \iint_{\mathbb{R}_+^2} p_t(s,b)\,\phi(s,b)\,\mathrm{d}s\,\mathrm{d}b\right\}\\ &\quad= \int_0^\infty q_t(s)\,\mathcal{L}\phi(s,0)\,\mathrm{d}s + \iint_{\mathbb{R}_+^2} p_t(s,b)\,\mathcal{L}\phi(s,b)\,\mathrm{d}s\,\mathrm{d}b\,.\end{aligned} \tag{11}$$

Lemma 3.1. *For all functions $\phi \in H^2_{\Gamma_2}(\mathbb{R}^2_+)$ (i.e. $\phi \in H^1(\mathbb{R}^2_+)$ and $\phi|_{\Gamma_2} = 0$) and $t \geq 0$*

$$\langle p_t, \mathcal{L}\phi\rangle = \int_{\mathbb{R}_+^2} \mathcal{L}^* p_t(x)\,\phi(x)\,\mathrm{d}x + \frac{c_2^2}{2}\int_0^\infty p_t(s,0)\,\phi(s,0)\,\mathrm{d}s$$

where $\mathcal{L}^*$ is the adjoint operator:

$$\mathcal{L}^*\psi(x) \stackrel{\text{def}}{=} -[\psi(x)\,f_1(x)]'_s - [\psi(x)\,f_2(x)]'_b + \frac{c_1^2}{2}\,[\psi(x)\,s]''_{s^2} + \frac{c_2^2}{2}\,[\psi(x)\,b]''_{b^2}\,.$$

Proof By definition of $\mathcal{L}$:

$$\begin{aligned}\langle p_t, \mathcal{L}\phi\rangle &= \int_{\mathbb{R}_+^2} p_t(x)\,\mathcal{L}\phi(x)\,\mathrm{d}x = \int_{\mathbb{R}_+^2} p_t(x)\,f_1(x)\,\phi'_s(x)\,\mathrm{d}x + \int_{\mathbb{R}_+^2} p_t(x)\,f_2(x)\,\phi'_b(x)\,\mathrm{d}x\\ &\quad + \frac{c_1^2}{2}\int_{\mathbb{R}_+^2} p_t(x)\,s\,\phi''_{s^2}(x)\,\mathrm{d}x + \frac{c_2^2}{2}\int_{\mathbb{R}_+^2} p_t(x)\,b\,\phi''_{b^2}(x)\,\mathrm{d}x.\end{aligned}$$

We consider separately these four last terms.

From Green's formula [1]: $\int_{\mathbb{R}_+^2} u'_{x_i}\,v\,\mathrm{d}x = -\int_{\mathbb{R}_+^2} u\,v'_{x_i}\,\mathrm{d}x + \int_{\partial\mathbb{R}_+^2} u\,v\,n_i\,\mathrm{d}\mathcal{S}_x$ where n_i is the ith component of the outward unit normal n, i.e. $n_1(x) = 0$ on Γ_1 and -1 on Γ_2 and $n_2(x) = -1$ on Γ_1 and 0 on Γ_2. So we get:

$$\begin{aligned}\int_{\mathbb{R}_+^2} p_t(x)\,f_1(x)\,\phi'_s(x)\,\mathrm{d}x &= -\int_{\mathbb{R}_+^2} [p_t(x)\,f_1(x)]'_s\,\phi(x)\,\mathrm{d}x + \int_{\partial\mathbb{R}_+^2} p_t(x)\,f_1(x)\,\phi(x)\,n_1(x)\,\mathrm{d}\mathcal{S}_x\\ &= -\int_{\mathbb{R}_+^2} [p_t(x)\,f_1(x)]'_s\,\phi(x)\,\mathrm{d}x - \int_{\Gamma_2} p_t(x)\,f_1(x)\,\phi(x)\,\mathrm{d}\mathcal{S}_x\\ &= -\int_{\mathbb{R}_+^2} [p_t(x)\,f_1(x)]'_s\,\phi(x)\,\mathrm{d}x\,. \quad (\text{as } \phi = 0 \text{ on } \Gamma_2)\end{aligned}$$

For the second term:

$$\begin{aligned}\int_{\mathbb{R}^2_+} p_t(x)\, f_2(x)\, \phi'_b(x)\, \mathrm{d}x &= -\int_{\mathbb{R}^2_+} [p_t(x)\, f_2(x)]'_b\, \phi(x)\, \mathrm{d}x + \int_{\partial\mathbb{R}^2_+} p_t(x)\, f_2(x)\, \phi(x)\, n_2(x)\, \mathrm{d}\mathcal{S}_x \\ &= -\int_{\mathbb{R}^2_+} [p_t(x)\, f_2(x)]'_b\, \phi(x)\, \mathrm{d}x - \int_{\Gamma_1} p_t(x)\, f_2(x)\, \phi(x)\, \mathrm{d}\mathcal{S}_x \\ &= -\int_{\mathbb{R}^2_+} [p_t(x)\, f_2(x)]'_b\, \phi(x)\, \mathrm{d}x\,. \quad (\text{as } f_2 = 0 \text{ on } \Gamma_1)\end{aligned}$$

For the third term:

$$\begin{aligned}\int_{\mathbb{R}^2_+} p_t(x)\, s\, \phi''_{s^2}(x)\, \mathrm{d}x &= -\int_{\mathbb{R}^2_+} [p_t(x)\, s]'_s\, \phi'_s(x)\, \mathrm{d}x + \int_{\partial\mathbb{R}^2_+} p_t(x)\, s\, \phi'_s(x)\, n_1(x)\, \mathrm{d}\mathcal{S}_x \\ &= -\int_{\mathbb{R}^2_+} [p_t(x)\, s]'_s\, \phi'_s(x)\, \mathrm{d}x - \int_{\Gamma_2} p_t(x)\, s\, \phi'_s(x)\, \mathrm{d}\mathcal{S}_x \\ &= -\int_{\mathbb{R}^2_+} [p_t(x)\, s]'_s\, \phi'_s(x)\, \mathrm{d}x \quad (\text{as } s = 0 \text{ on } \Gamma_2) \qquad = \int_{\mathbb{R}^2_+} [p_t(x)\, s]''_{s^2}\, \phi(x)\, \mathrm{d}x \\ &\qquad\qquad - \int_{\partial\mathbb{R}^2_+} [p_t(x)\, s]'_s\, \phi(x)\, n_1(x)\, \mathrm{d}\mathcal{S}_x \\ &= \int_{\mathbb{R}^2_+} [p_t(x)\, s]''_{s^2}\, \phi(x)\, \mathrm{d}x + \int_{\Gamma_2} [p_t(x)\, s]'_s\, \phi(x)\, \mathrm{d}\mathcal{S}_x \\ &= \int_{\mathbb{R}^2_+} [p_t(x)\, s]''_{s^2}\, \phi(x)\, \mathrm{d}x\,. \quad (\text{as } \phi = 0 \text{ on } \Gamma_2)\end{aligned}$$

For the fourth term:

$$\begin{aligned}\int_{\mathbb{R}^2_+} p_t(x)\, b\, \phi''_{b^2}(x)\, \mathrm{d}x &= -\int_{\mathbb{R}^2_+} [p_t(x)\, b]'_b\, \phi'_b(x)\, \mathrm{d}x + \int_{\partial\mathbb{R}^2_+} p_t(x)\, b\, \phi'_b(x)\, n_2(x)\, \mathrm{d}\mathcal{S}_x \\ &= -\int_{\mathbb{R}^2_+} [p_t(x)\, b]'_b\, \phi'_b(x)\, \mathrm{d}x - \int_{\Gamma_1} p_t(x)\, b\, \phi'_b(x)\, \mathrm{d}\mathcal{S}_x \\ &= -\int_{\mathbb{R}^2_+} [p_t(x)\, b]'_b\, \phi'_b(x)\, \mathrm{d}x \quad (\text{as } b = 0 \text{ on } \Gamma_1) \qquad = \int_{\mathbb{R}^2_+} [p_t(x)\, b]''_{b^2}\, \phi(x)\, \mathrm{d}x \\ &\qquad\qquad - \int_{\partial\mathbb{R}^2_+} [p_t(x)\, b]'_b\, \phi(x)\, n_2(x)\, \mathrm{d}\mathcal{S}_x \\ &= \int_{\mathbb{R}^2_+} [p_t(x)\, b]''_{b^2}\, \phi(x)\, \mathrm{d}x + \int_{\Gamma_1} [p_t(x)\, b]'_b\, \phi(x)\, \mathrm{d}\mathcal{S}_x\,.\end{aligned}$$

Summing up these identities leads to:

$$\langle p_t, \mathcal{L}\phi\rangle = \langle \mathcal{L}^*\, p_t, \phi\rangle + \frac{c_2^2}{2} \int_{\Gamma_1} [p_t(x)\, b]'_b\, \phi(x)\, \mathrm{d}\mathcal{S}_x\,,$$

and finally

$$\begin{aligned}\int_{\Gamma_1} [p_t(x)\, b]'_b\, \phi(x)\ \mathrm{d}\mathcal{S}_x &= \int_{\Gamma_1} \{[p_t(x)]'_b\, b + p_t(x)\}\, \phi(x)\ \mathrm{d}\mathcal{S}_x \\ &= \int_{\Gamma_1} p_t(x)\, \phi(x)\ \mathrm{d}\mathcal{S}_x \\ &= \int_0^\infty p_t(s,0)\, \phi(s,0)\ \mathrm{d}s\end{aligned}$$

proves the lemma. □

According to Lemma 3.1, (11) becomes:

$$\begin{aligned}&\frac{\mathrm{d}}{\mathrm{d}t}\left\{\int_0^\infty q_t(s)\, \phi(s,0)\, \mathrm{d}s + \iint_{\mathbb{R}_+^2} p_t(s,b)\, \phi(s,b)\, \mathrm{d}s\, \mathrm{d}b\right\} \\ &\quad = \int_0^\infty q_t(s)\, \mathcal{L}\phi(s,0)\, \mathrm{d}s + \iint_{\mathbb{R}_+^2} \mathcal{L}^* p_t(s,b)\, \phi(s,b)\, \mathrm{d}s\, \mathrm{d}b + \frac{c_2^2}{2}\int_0^\infty p_t(s,0)\, \phi(s,0)\, \mathrm{d}s\,. \end{aligned} \tag{12}$$

Let $\phi(s,b) = \varphi(s)\,\psi(b)$ with $\psi(0)=1$, $\psi(b)=0$ for $b>\varepsilon$ and $\psi'(0)=\psi''(0)=0$, after letting $\varepsilon\to 0$, the previous equation leads to:

$$\frac{\mathrm{d}}{\mathrm{d}t}\int_0^\infty q_t(s)\, \varphi(s)\, \mathrm{d}s = \int_0^\infty q_t(s)\, \mathcal{G}\varphi(s)\, \mathrm{d}s + \frac{c_2^2}{2}\int_0^\infty p_t(s,0)\, \varphi(s)\, \mathrm{d}s \tag{13}$$

where

$$\mathcal{G}\varphi(s) = D\,(s_{\mathrm{in}} - s)\,\varphi'(s) + \frac{c_2^2}{2}\, s\, \varphi''(s) \tag{14}$$

is the infinitesimal generator of the diffusion S_t in washout mode, i.e. of the SDE (6). As (13) is valid for all test functions φ, we get the following equation for $q_t(s)$:

$$\frac{\partial}{\partial t} q_t(s) = \mathcal{G}^* q_t(s) + \frac{c_2^2}{2}\, p_t(s,0), \quad \forall t \geq 0\,, \quad s \in [0,\infty)\,, \tag{15a}$$

the equation for $p_t(s,b)$ is

$$\frac{\partial}{\partial t} p_t(s,b) = \mathcal{L}^* p_t(s,b), \quad \forall t \geq 0\,, \quad (s,b) \in [0,\infty)^2\,. \tag{15b}$$

The initial condition for (15a) and (15b) are:

$$q_t(s) = \rho_{\mathrm{v}}(s), \qquad p_t(s,v) = \rho(s,b) \tag{15c}$$

where $\rho_{\mathrm{v}}(s)\,\mathrm{d}s\,\delta_0(\mathrm{d}b) + \rho(s,b)\,\mathrm{d}s\,\mathrm{d}b$ is the distribution law of $X_0 = (S_0, B_0)$.

The operators are:

$$\mathcal{G}^*\varphi(s) = -D\,[(s_{\mathrm{in}} - s)\,\varphi(s)]' + \frac{c_2^2}{2}\,[s\,\varphi(s)]''\,, \tag{16}$$

$$\mathcal{L}^*\phi(s,b) = -[f_1(s,b)\,\phi(s,b)]'_s - [f_2(s,b)\,\phi(s,b)]'_b + \frac{c_1^2}{2}\,[s\,\phi(s,b)]''_{s^2} + \frac{c_2^2}{2}\,[b\,\phi(s,b)]''_{b^2}\,. \tag{17}$$

Finally, the Fokker–Planck equation is a system of PDE's: (15b) for $p_t(s,v)$ and (15a) for $q_t(s)$, the first one is autonomous, and its solution appears as an input for the second PDE.

4. Approximation

Many finite difference schemes and finite element schemes are adapted to space discretization of the system (15). Here we use the specific finite difference scheme proposed in [8]. This classical scheme presents nice numerical properties and it also can be interpreted as an approximation of the solution of (4) by a pure jump Markov process on a finite discretization grid, the resulting system in discrete-space and continuous-time is the exact Fokker–Planck equation (forward Kolmogorov equation) associated with this pure jump process. The infinitesimal generator $\mathcal{L}$ of the SDE (4) is given by (10), this operator fully characterizes the distribution law of the process $X_t = (S_t, B_t)$, indeed the set of equations (15) is totally determined by the operator $\mathcal{L}$ as $\mathcal{G}$ is only the restriction of $\mathcal{L}$ to Γ_2.

The finite difference scheme is detailed in Appendix A, it leads to the following approximation of the infinitesimal generator:

$$\mathcal{L}\phi(x) \simeq \mathcal{L}_h\phi(x) = \sum_{y\in G_h} \mathcal{L}_h(x, y)\,\phi(y)$$

for $x \in G_h$ where:

$$\begin{aligned} G_h &\stackrel{\text{def}}{=} \{x = (k_1\,h_1, k_2\,h_2)\,;\, k_i = 0, \ldots, N_i,\ i = 1, 2\},\\ \overset{\circ}{G}_h &\stackrel{\text{def}}{=} \{x = (k_1\,h_1, k_2\,h_2)\,;\, k_i = 1, \ldots, N_i - 1,\ i = 1, 2\}\,,\\ G_h^1 &\stackrel{\text{def}}{=} \{x = (k_1\,h_1, 0)\,;\, k_1 = 0, \ldots, N_1\}\,, \end{aligned}$$

are the grid version of $\mathbb{R}^2_+$, $\overset{\circ}{\mathbb{R}}{}^2_+$ and Γ_1 respectively, see Fig. 1.

For the interior points $x \in \overset{\circ}{G}_h$ the finite difference scheme is:

$$\begin{cases} \mathcal{L}_h(x, x) & = -\dfrac{|f_1(x)|}{h_1} - \dfrac{|f_2(x)|}{h_2} - \dfrac{\sigma_1^2(x)}{h_1^2} - \dfrac{\sigma_2^2(x)}{h_2^2}\,,\\ \mathcal{L}_h(x, x \pm h_i\,e_i) & = \dfrac{f_i^{\pm}(x)}{h_i} + \dfrac{\sigma_i^2(x)}{2\,h_i^2}\,, \quad i = 1, 2\,,\\ \mathcal{L}_h(x, y) & = 0 \qquad \text{otherwise.} \end{cases}$$

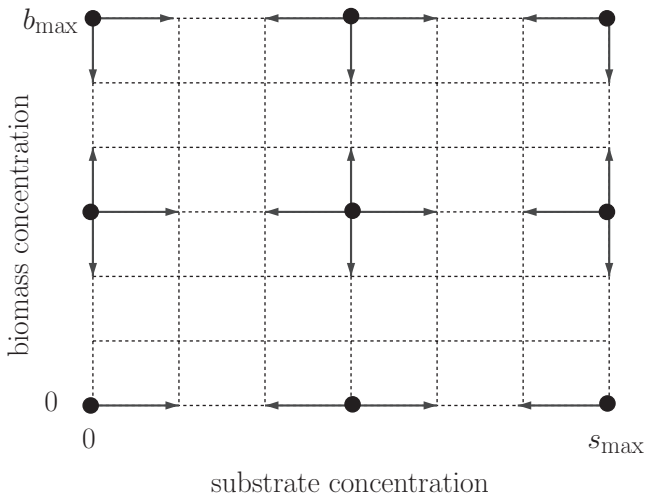

Fig. 1. Discretized domain G_h.

For the boundary points $x \in G_h \setminus \overset{\circ}{G}_h$ the finite difference schemes are detailed in Appendix B. They correspond to Fig. 1: for $s = s_{\max}$ or $b = b_{\max}$, we must impose reflecting conditions, for $s = 0$ or $b = 0$, the boundary conditions are natural, they derive from the value of the coefficients. Indeed, when $b = 0$, then $f_2 = \sigma_2 = 0$ and the jump process stays on the boundary "$b = 0$" (it cannot jump to $b = h_2$ or to $b = -h_2$). When $s = 0$, then $f_1 = D\, s_{\text{in}}$ and $\sigma_1 = 0$, so the jump process can only jump to $s = h_1$.

We obtain a matrix $\mathcal{L}_h = [\mathcal{L}_h(x, y)]_{x,y \in G_h}$ which is the infinitesimal generator of a pure jump Markov process $(X_t^h)_{t \geq 0}$ in continuous time and discrete state space G_h. Starting from a point x of the grid, the process X_t^h stays

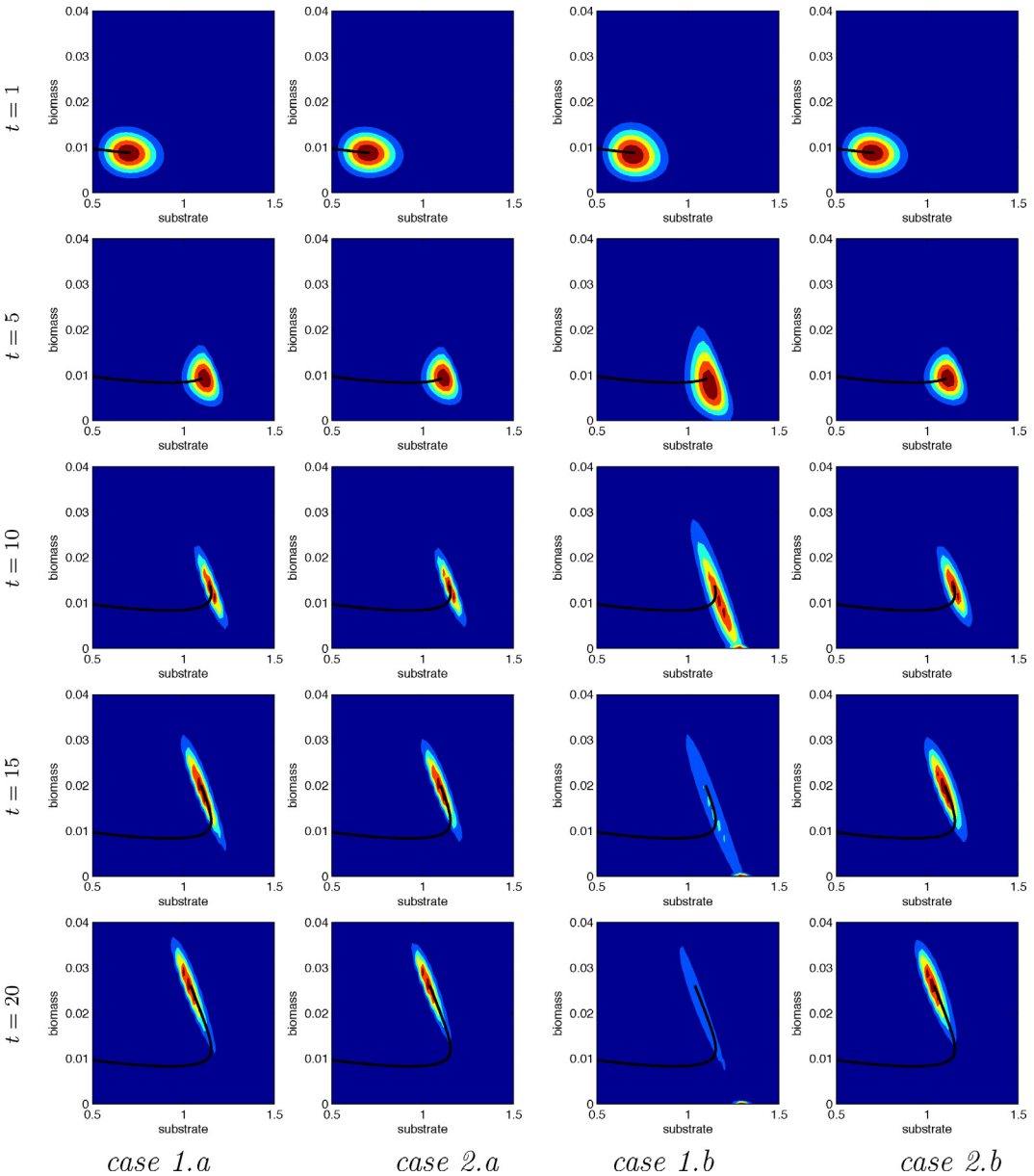

Fig. 2. In cases "1" the diffusion coefficients are $\sigma_1(s) = c_1 \sqrt{s}$ and $\sigma_2(b) = c_2 \sqrt{b}$; in cases "2" the diffusion coefficients are $\sigma_1(s) = c_1\, s$ and $\sigma_2(b) = c_2\, b$. In cases "a" $c_1 = c_2 = 0.005$; in cases "b" $c_1 = c_2 = 0.02$. For small noise intensities (case "a"), cases "1" and "2" behave rather similarly. For higher noise intensities (case "b"), as the law π_t of (S_t, B_t) is closer to the absorbing "washout" boundary $\{(s, b) \in \mathbb{R}_+^2 ; b = 0\}$, cases "1" and "2" behave rather similarly. See Fig. 3 for the evaluation of the washout probability.

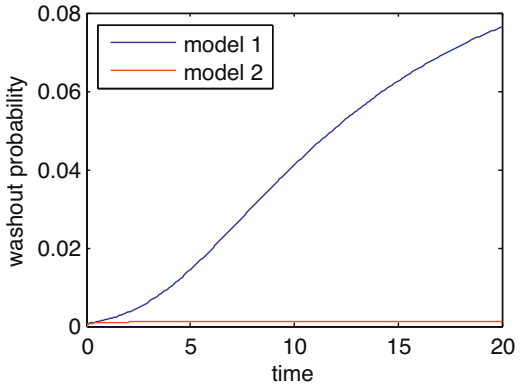

Fig. 3. Washout probability—following Fig. 2: we compute $t \to \mathbb{P}(B_t = 0)$ for the case "1" (model 1: $\sigma_1(s) = c_1\sqrt{s}$, $\sigma_2(b) = c_2\sqrt{b}$) and for case "2" (model 2: $\sigma_1(s) = c_1 s$, $\sigma_2(b) = c_2 b$).

there during a time exponentially distributed with parameter $-\mathcal{L}_h(x, x)$ then it jumps to a point y with probability $\mathcal{L}_h(x, y)/(-\mathcal{L}_h(x, x))$ for all $y \in \mathcal{G}_h$, and $\mathcal{L}_h$ is a $\mathcal{Q}$-matrix as $\sum_{y\in\mathcal{G}_h} \mathcal{L}_h(x, y) = 0$. Then the following Kolmogorov forward equation:

$$\frac{\partial}{\partial t} p_t^h(x) = \mathcal{L}_h^* \, p_t^h(x) \tag{18}$$

gives the evolution of the distribution law p_t^h of X_t^h, $p_t^h(x) = \mathbb{P}(X_t^h = x)$, $x \in G_h$.

It is important to note that this approach gives an approximation of the coupled system of PDEs (15): $(p_t^h(x))_{x\in G_h\setminus G_h^1}$ is an approximation of $(p_t(s, b))_{(s,b)\in(0,\infty)^2}$ and $(p_t^h(x))_{x\in G_h^1}$ is an approximation of $(q_t(s))_{s\in(0,\infty)}$.

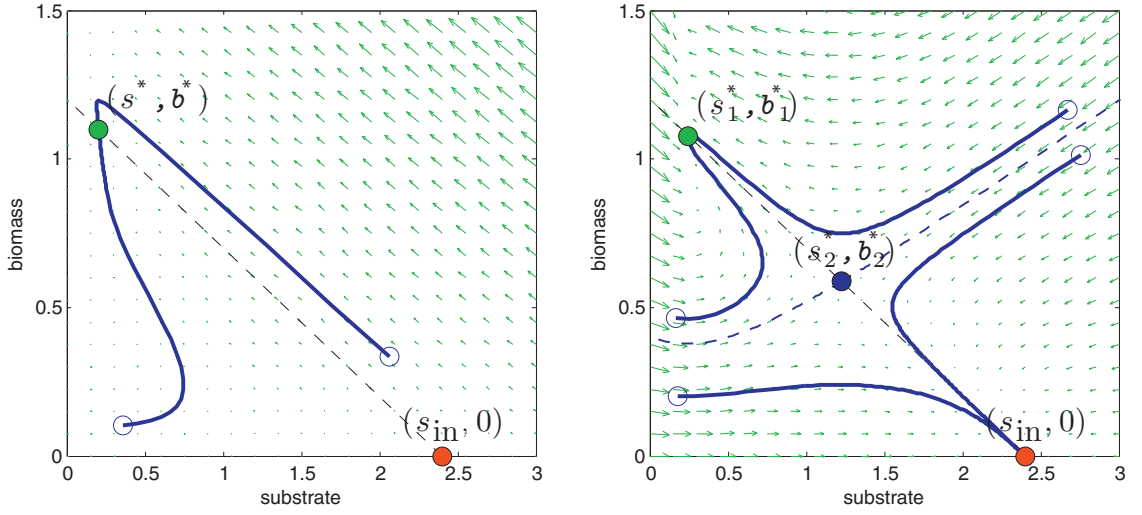

Fig. 4. Phase portraits for the system (1) for the Monod growth function (left) and the Haldane growth function. **Left (Monod case)**: there are two equilibrium states: the washout equilibrium (red dot) is unattractive, the equilibrium point (s^*, b^*) with $s^* = k_s D/(\mu_{\max} - D)$ (solution of $\mu(s) = D$) and $b^* = (s_{\text{in}} - s^*)/k$ is attractive. We suppose that $\mu_{\max} > D$. The dashed line is $b = (s_{\text{in}} - s)/k$, in blue two trajectories (blue circles: initial positions). **Right (Haldane case)**: the washout is still an equilibrium point but now it is attractive, there are two other equilibrium points given as solutions of $\mu(s) = D$ (we suppose that it admits two separate solutions), (s_1^*, b_1^*) is attractive (corresponding to the smallest value of s), (s_2^*, b_2^*) is unattractive. The black dashed curve separates the two basins of attraction; in blue four trajectories (blue circles: initial positions). (For interpretation of the references to color in this figure legend, the reader is referred to the web version of the article.)

For the time-discretization we use the implicit Euler scheme approximation:

$$\frac{p^h_{t+\delta}(x) - p^h_t(x)}{\delta} = \mathcal{L}^*_h\, p^h_{t+\delta}(x)$$

that is:

$$(I - \delta\, \mathcal{L}^*_h)\, p_{t+\delta}(x) = p_t(x)\,.$$

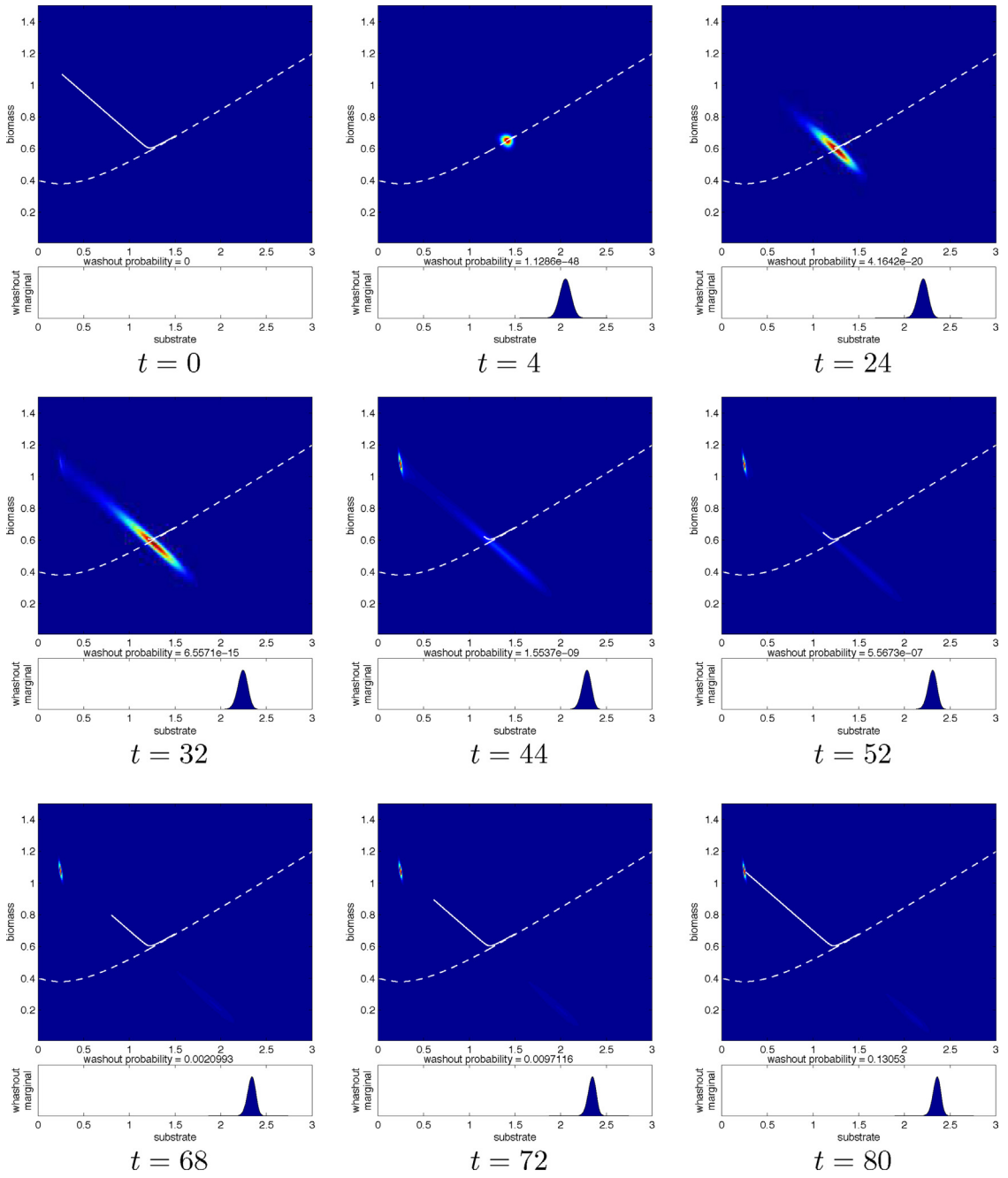

Fig. 5. Evolution of the distribution law of X_t: for each time t, the density $p_t(s, b)$ together with the washout density $q_t(s)$; the dashed curve separates the two basins of attraction. The mean of X_0 is on this curve. See comments in the text.

5. Numerical results

5.1. Comparison

Many works [6] propose the following structure for the diffusion coefficients:

$$\mathrm{d}S_t = \{-k\,\mu(S_t)\,B_t + D\,(s_{\mathrm{in}} - S_t)\}\,\mathrm{d}t + c_1\,S_t\,\mathrm{d}W_t^1\,, \tag{19a}$$

$$\mathrm{d}B_t = \{\mu(S_t)\,B_t - D\,B_t\}\,\mathrm{d}t + c_2\,B_t\,\mathrm{d}W_t^2\,. \tag{19b}$$

It is slightly different from (4). In large population size, these two models are rather equivalent; they differ drastically in the washout regime.

The solution of the Fokker–Planck equation associated with system (19) is approximated using the same discretization approach described in Section 4. However, the treatment of the boundary condition is simplified as process (19) never reaches the boundary [6].

In this test we use the Monod growth rate function (2) and the parameters: $k=10$, $s_{\mathrm{in}}=1.3$ (mg/l), $D=0.4$ (1/h), $\mu_{\max}=3$ (1/h), $k_s=6$ (mg/l). The initial law is $(S_0,\,B_0)\sim\mathcal{N}(0.45,\,10^{-5})\otimes\mathcal{N}(0.01,\,10^{-5})$. The discretization parameters are $s_{\max}=2$, $b_{\max}=0.06$, $\delta=0.1$, $N_1=N_2=70$. In Fig. 2, we see that with small noise intensities the simulation of the two models are very similar; with higher noise intensity, the simulations are very different. This is due to the fact that the behavior of the two diffusion processes near the boundary "$b=0$" are different: with the model (4) the washout regime is attainable which is not the case with the model (19). In Fig. 3 we compare the evolution of the washout probability $t\to\mathbb{P}(B_t=0)$ for both models, we clearly see that the model (10) does not give account for this probability.

5.2. Simulation with the Haldane growth rate function

In this test we use the Haldane growth rate function (3) and the parameters: $k=2$, $s_{\mathrm{in}}=2.4$ (mg/l), $D=0.1$ (1/h), $\overline{\mu}=5$ (1/h), $k_s=10$ (mg/l), $\alpha=0.03$: $c_1=c_2=0.01$. The initial law is $(S_0,\,B_0)\sim\mathcal{N}(1.5,\,10^{-5})\otimes\mathcal{N}(0.68,\,10^{-5})$. The discretization parameters are $s_{\max}=3$, $b_{\max}=2.5$, $\delta=0.25$, $N_1=N_2=300$.

In Fig. 5 we plot the time evolution of the distribution law of X_t: for each time t, we represent (the approximation of) $(p_t(s,\,b)\,;(s,\,b)\in(0,\,s_{\max})\times(0,\,b_{\max}))$ together with (the approximation of) $(q_t(s)\,;s\in(0,\,s_{\max}))$. In this test the mean of X_0 is on this curve that separates the two basins of attraction (dashed white line): hence part of the mass will be attracted by $(s_1^*,\,b_1^*)$ and the other part will be attracted by the washout $(s_{\mathrm{in}},\,0)$ (see Figs. 4 and 5).

For $t=0$ we plot all the trajectory $(x(t))_{t\in[0;80]}$ (white line). At the beginning the distribution law starts to "stretch" between the two attractors ($t=24$). At $t=32$, part of the mass is already on the point $(s_1^*,\,b_1^*)$. Note that at this instant $p_t(s,\,b)$ is bimodal and $x(t)$ is a good approximation of $\mathbb{E}(X_t)$, but it is a poor statistics for X_t. At the final time $t=80$, the deterministic trajectory $x(t)$ reaches the equilibrium point $(s_1^*,\,b_1^*)$ and 13% of the mass has been trapped by the washout absorbing boundary and some mass is still in the washout basin and will be trapped by the boundary "$b=0$".

Acknowledgement

The work was partially supported by the French National Research Agency (ANR) within the SYSCOMM project ANR-09- SYSC-003.

Appendix A. General finite difference scheme for n-dimensional diffusion processes

Let X_t be the following diffusion process:

$$\mathrm{d}X_t \quad = b(X_t)\,\mathrm{d}t + \sigma(X_t)\,\mathrm{d}W_t$$

where X_t takes values in $\mathbb{R}^n$, $b:\mathbb{R}^n\mapsto\mathbb{R}^n$, $\sigma:\mathbb{R}^n\mapsto\mathbb{R}^{n\times m}$, and W_t is a standard Brownian motion with values in $\mathbb{R}^m$. Let $a=\sigma\,\sigma^*:\mathbb{R}^n\mapsto\mathbb{R}^{n\times n}$. The coefficients b and σ are supposed to be locally Lipschitz and at most of linear growth.

The probability density function $p(t, x)$ of X_t is solution of the following Fokker–Planck equation:

$$\frac{\partial}{\partial t}\, p(t,x) = \mathcal{L}^* p(t,x) \tag{A.1}$$

where $\mathcal{L}$ is the infinitesimal generator defined by:

$$\mathcal{L}\phi(x) \quad \stackrel{\text{def}}{=} \sum_{i=1}^{n} f_i(x)\, \phi'_{x_i}(x) + \frac{1}{2} \sum_{i,j=1}^{n} a_{ij}(x)\, \phi''_{x_i x_j}(x)\,.$$

We consider finite difference schemes based on the following stencil (for the components (x_i, x_j)):

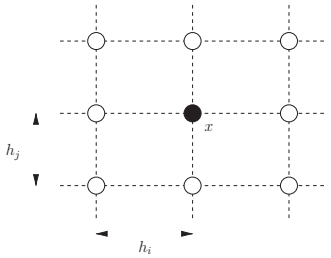

We use the following up-wind scheme [8,9]:

$$f_i(x)\,\phi'_{x_i}(x) \quad \simeq \begin{cases} f_i(x)\,\dfrac{\phi(x+h_i\,e_i)-\phi(x)}{h_i}\,, & \text{if } f_i(x)\geq 0\,,\\ f_i(x)\,\dfrac{\phi(x)-\phi(x-h_i\,e_i)}{h_i}\,, & \text{if } f_i(x)<0\,, \end{cases}$$

$$a_{ii}(x)\,\phi''_{x_i^2}(x) \quad \simeq a_{ii}(x)\,\frac{\phi(x+h_i\,e_i)-2\,\phi(x)+\phi(x-h_i\,e_i)}{h_i^2}\,,$$

$$a_{ij}(x)\,\phi''_{x_i x_j}(x) \quad \simeq \begin{cases} a_{ij}(x)\,\dfrac{1}{2\,h_i}\left[\dfrac{\phi(x+h_i\,e_i+h_j\,e_j)-\phi(x+h_i\,e_i)}{h_j} - \dfrac{\phi(x+h_j\,e_j)-\phi(x)}{h_j}\right.\\ \qquad \left. +\dfrac{\phi(x)-\phi(x-h_j\,e_j)}{h_j} - \dfrac{\phi(x-h_i\,e_i)-\phi(x-h_i\,e_i-h_j\,e_j)}{h_j}\right]\,, & \text{if } a_{ij}(x)\geq 0,\\ a_{ij}(x)\,\dfrac{1}{2\,h_i}\left[\dfrac{\phi(x+h_i\,e_i)-\phi(x+h_i\,e_i-h_j\,e_j)}{h_j} - \dfrac{\phi(x)-\phi(x-h_j\,e_j)}{h_j}\right.\\ \qquad \left. +\dfrac{\phi(x+h_j\,e_j)-\phi(x)}{h_j} - \dfrac{\phi(x-h_i\,e_i+h_j\,e_j)-\phi(x-h_i\,e_i)}{h_j}\right]\,, & \text{if } a_{ij}(x)<0\,, \end{cases}$$

for $i, j = 1, \ldots, n$, $i \neq j$. The last non-diagonal second order schemes correspond to the following diagrams:

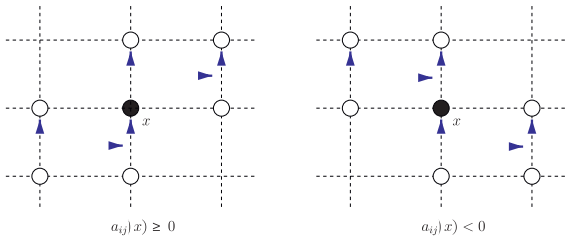

With notation $f^{+}(x) = \max(f(x), 0)$ and $f^{-}(x) = \max(-f(x), 0)$, we get the following approximation:

$$
\begin{aligned}
\mathcal{L}_h\phi(x) &= \sum_i f_i(x)\,\phi'_{x_i}(x) + \frac{1}{2}\sum_{i,j} a_{i,j}(x)\,\phi''_{x_i x_j}(x) \\
&= \sum_i \{f_i^+(x) - f_i^-(x)\}\,\phi'_{x_i}(x) + \frac{1}{2}\sum_i a_{ii}(x)\,\phi''_{x_i^2}(x) + \frac{1}{2}\sum_{i,j;i\neq j} \{a_{ij}^+(x) - a_{ij}^-(x)\}\,\phi''_{x_i x_j}(x) \\
&\simeq \sum_i \left\{ \frac{f_i^+(x)}{h_i}\,[\phi(x + h_i\,e_i) - \phi(x)] - \frac{f_i^-(x)}{h_i}\,[\phi(x) - \phi(x - h_i\,e_i)] \right\} \\
&\quad + \sum_i \frac{a_{ii}(x)}{2\,h_i^2}\,[\phi(x + h_i\,e_i) - 2\,\phi(x) + \phi(x - h_i\,e_i)] \\
&\quad + \frac{1}{2}\sum_{i,j;i\neq j} \left\{ \frac{a_{ij}^+(x)}{2\,h_i\,h_j}\,\big([\phi(x + h_i\,e_i + h_j\,e_j) - \phi(x + h_i\,e_i)] \right. \\
&\quad -[\phi(x + h_j\,e_j) - \phi(x)] + [\phi(x) - \phi(x - h_j\,e_j)] \\
&\quad \left. -[\phi(x - h_i\,e_i) - \phi(x - h_i\,e_i - h_j\,e_j)]\big) \right. \\
&\quad - \frac{a_{ij}^-(x)}{2\,h_i\,h_j}\,\big([\phi(x + h_i\,e_i) - \phi(x + h_i\,e_i - h_j\,e_j)] \\
&\quad -[\phi(x) - \phi(x - h_j\,e_j)] + [\phi(x + h_j\,e_j) - \phi(x)] \\
&\quad \left. -[\phi(x - h_i\,e_i + h_j\,e_j) - \phi(x - h_i\,e_i)]\big) \right\} \\
&= \phi(x) \left\{ -\sum_i \frac{|f_i(x)|}{h_i} - \sum_i \frac{a_{ii}(x)}{h_i^2} + \sum_{i,j;i\neq j} \frac{|a_{ij}(x)|}{2\,h_i\,h_j} \right\} \\
&\quad + \sum_i \phi(x + h_i\,e_i) \quad \left\{ \frac{f_i^+(x)}{h_i} + \frac{a_{ii}(x)}{2\,h_i^2} - \sum_{j;j\neq i} \frac{|a_{ij}(x)|}{4\,h_i\,h_j} \right\} \\
&\quad + \sum_j \sum_{i;i\neq j} \phi(x + h_j\,e_j) \quad \frac{|a_{ij}(x)|}{4\,h_i\,h_j} \\
&\quad + \sum_i \phi(x - h_i\,e_i) \quad \left\{ \frac{f_i^-(x)}{h_i} + \frac{a_{ii}(x)}{2\,h_i^2} - \sum_{j;j\neq i} \frac{|a_{ij}(x)|}{4\,h_i\,h_j} \right\} \\
&\quad + \sum_j \sum_{i;i\neq j} \phi(x - h_j\,e_j) \quad \frac{|a_{ij}(x)|}{4\,h_i\,h_j} \\
&\quad + \sum_{i,j;i\neq j} \left\{ \frac{a_{ij}^+(x)}{2\,h_i\,h_j}\,[\phi(x + h_i\,e_i + h_j\,e_j) + \phi(x - h_i\,e_i - h_j\,e_j)] \right. \\
&\quad \left. + \frac{a_{ij}^-(x)}{2\,h_i\,h_j}[\phi(x + h_i\,e_i - h_j\,e_j) + \phi(x - h_i\,e_i + h_j\,e_j)] \right\}
\end{aligned}
$$

the symmetry $a_{ij} = a_{ji}$ leads to

$$\begin{aligned}
\mathcal{L}_h\phi(x) \quad &= \phi(x) \quad \left\{ -\sum_i \frac{|f_i(x)|}{h_i} - \sum_i \frac{a_{ii}(x)}{h_i^2} + \sum_{i,j;i\neq j} \frac{|a_{ij}(x)|}{2\,h_i\,h_j} \right\} \\
&+ \sum_i \phi(x + h_i\,e_i) \quad \left\{ \frac{f_i^+(x)}{h_i} + \frac{a_{ii}(x)}{2\,h_i^2} - \sum_{j;j\neq i} \frac{|a_{ij}(x)|}{2\,h_i\,h_j} \right\} \\
&+ \sum_i \phi(x - h_i\,e_i) \quad \left\{ \frac{f_i^-(x)}{h_i} + \frac{a_{ii}(x)}{2\,h_i^2} - \sum_{j;j\neq i} \frac{|a_{ij}(x)|}{2\,h_i\,h_j} \right\} \\
&+ \sum_{i,j;i\neq j} \left\{ \frac{a_{ij}^+(x)}{2\,h_i\,h_j} [\phi(x + h_i\,e_i + h_j\,e_j) + \phi(x - h_i\,e_i - h_j\,e_j)] \right. \\
&\left. + \frac{a_{ij}^-(x)}{2\,h_i\,h_j} [\phi(x + h_i\,e_i - h_j\,e_j) + \phi(x - h_i\,e_i + h_j\,e_j)] \right\}.
\end{aligned}$$

We get the following approximation of the infinitesimal generator:

$$\mathcal{L}\phi(x) \simeq \mathcal{L}_h\phi(x) = \sum_{y\in G_h} \mathcal{L}_h(x, y)\,\phi(y)$$

for $x \in G_h$ where $G_h = \{x = (k_1\,h_1, \ldots, k_n\,h_n)\,; k_i = 0, \ldots, N_i, i = 1, \ldots, n\}$ and

$$\begin{cases}
\mathcal{L}_h(x, x) & = -\sum_{i=1}^n \frac{|f_i(x)|}{h_i} - \sum_{i=1}^n \{\frac{a_{ii}(x)}{h_i^2} - \sum_{j\neq i} \frac{|a_{ij}(x)|}{2\,h_i\,h_j}\}, \\
\mathcal{L}_h(x, x \pm h_i\,e_i) & = \frac{f_i^\pm(x)}{h_i} + \frac{a_{ii}(x)}{2\,h_i^2} - \sum_{j;j\neq i} \frac{|a_{ij}(x)|}{2\,h_i\,h_j}, \\
\mathcal{L}_h(x, x + h_i\,e_i + h_j\,e_j) & = \mathcal{L}_h(x, x - h_i\,e_i - h_j\,e_j) = \frac{a_{ij}^+(x)}{2\,h_i\,h_j} \qquad \text{for } i \neq j, \\
\mathcal{L}_h(x, x + h_i\,e_i - h_j\,e_j) & = \mathcal{L}_h(x, x - h_i\,e_i + h_j\,e_j) = \frac{a_{ij}^-(x)}{2\,h_i\,h_j} \qquad \text{for } i \neq j, \\
\mathcal{L}_h(x, y) & = 0 \qquad \text{otherwise.}
\end{cases}$$

Appendix B. Boundary conditions for the finite difference approximation

For the boundary points $G_h \setminus \overset{\circ}{G}_h$ of the grid, we use the following schemes:

- For $x \in \{(s, b) \in G_h \,;\, s = 0,\, b \in (0, b_{\max})\}$

$$\begin{cases} \mathcal{L}_h(x, x) & = -\dfrac{|f_1(x)|}{h_1} - \dfrac{|f_2(x)|}{h_2} - \dfrac{\sigma_1^2(x)}{h_1^2} - \dfrac{\sigma_2^2(x)}{h_2^2}\,, \\ \mathcal{L}_h(x, x + h_1\, e_1) & = \dfrac{f_1^+(x)}{h_1} + \dfrac{\sigma_1^2(x)}{2\,h_1^2}\,, \\ \mathcal{L}_h(x, x - h_1\, e_1) & = \dfrac{f_1^-(x)}{h_1} + \dfrac{\sigma_1^2(x)}{2\,h_1^2} = 0 \text{ because } f_1(0, b) = D\, s_{\text{in}}\,, \quad \sigma_1(0, b) = 0\,, \\ \mathcal{L}_h(x, x \pm h_2\, e_2) & = \dfrac{f_2^{\pm}(x)}{h_2} + \dfrac{\sigma_2^2(x)}{2\,h_2^2}\,, \text{ note that } f_2(0, b) = -D\, b < 0\,, \\ \mathcal{L}_h(x, y) & = 0 \qquad \text{otherwise.} \end{cases}$$

- For $x \in \{(s, b) \in G_h \,;\, s = s_{\max},\, b \in (0, b_{\max})\}$

$$\begin{cases} \mathcal{L}_h(x, x) & = -\dfrac{|f_1(x)|}{h_1} - \dfrac{|f_2(x)|}{h_2} - \dfrac{\sigma_1^2(x)}{h_1^2} - \dfrac{\sigma_2^2(x)}{h_2^2}\,, \\ \mathcal{L}_h(x, x + h_1\, e_1) & = 0 \text{ (set artificially to 0)}\,, \\ \mathcal{L}_h(x, x - h_1\, e_1) & = \dfrac{|f_1(x)|}{h_1} + \dfrac{\sigma_1^2(x)}{h_1^2}\,, \\ \mathcal{L}_h(x, x \pm h_2\, e_2) & = \dfrac{f_2^{\pm}(x)}{h_2} + \dfrac{\sigma_2^2(x)}{2\,h_2^2}\,, \\ \mathcal{L}_h(x, y) & = 0 \qquad \text{otherwise.} \end{cases}$$

- For $x \in \{(s, b) \in G_h \,;\, s \in (0, s_{\max}),\, b = 0\}$

$$\begin{cases} \mathcal{L}_h(x, x) & = -\dfrac{|f_1(x)|}{h_1} - \dfrac{\sigma_1^2(x)}{h_1^2}\,, \\ \mathcal{L}_h(x, x \pm h_1\, e_1) & = \dfrac{f_1^{\pm}(x)}{h_1} + \dfrac{\sigma_1^2(x)}{2\,h_1^2}\,, \\ \mathcal{L}_h(x, x \pm h_2\, e_2) & = \dfrac{f_2^{\pm}(x)}{h_2} + \dfrac{\sigma_2^2(x)}{2\,h_2^2} = 0 \text{ because } f_2(s, 0) = \sigma_2(s, 0) = 0\,, \\ \mathcal{L}_h(x, y) & = 0 \qquad \text{otherwise.} \end{cases}$$

- For $x \in \{(s, b) \in G_h \,;\, s \in (0, s_{\max}),\, b = b_{\max}\}$

$$\begin{cases} \mathcal{L}_h(x, x) & = -\dfrac{|f_1(x)|}{h_1} - \dfrac{|f_2(x)|}{h_2} - \dfrac{\sigma_1^2(x)}{h_1^2} - \dfrac{\sigma_2^2(x)}{h_2^2}\,, \\ \mathcal{L}_h(x, x \pm h_1\, e_1) & = \dfrac{f_1^{\pm}(x)}{h_1} + \dfrac{\sigma_1^2(x)}{2\, h_1^2}\,, \\ \mathcal{L}_h(x, x + h_2\, e_2) & = 0 \text{ (set artificially to 0)}\,, \\ \mathcal{L}_h(x, x - h_2\, e_2) & = \dfrac{|f_2(x)|}{h_2} + \dfrac{\sigma_2^2(x)}{h_2^2}\,, \\ \mathcal{L}_h(x, y) & = 0 \qquad \text{otherwise.} \end{cases}$$

- For $x = (0, 0)$

$$\begin{cases} \mathcal{L}_h(x, x) & = -\dfrac{|f_1(x)|}{h_1}\,, \\ \mathcal{L}_h(x, x + h_1\, e_1) & = \dfrac{f_1^{+}(x)}{h_1}\,, \\ \mathcal{L}_h(x, x - h_1\, e_1) & = 0 \text{ because } f_1(0,0) = D\, s_{\text{in}}\,, \quad \sigma_1(0,0) = 0\,,\,, \\ \mathcal{L}_h(x, x \pm h_2\, e_2) & = 0 \text{ because } f_2(0,0) = \sigma_2(0,0) = 0\,, \\ \mathcal{L}_h(x, y) & = 0 \qquad \text{otherwise.} \end{cases}$$

- For $x = (s_{\max}, 0)$

$$\begin{cases} \mathcal{L}_h(x, x) & = -\dfrac{|f_1(x)|}{h_1} - \dfrac{\sigma_1^2(x)}{h_1^2}\,, \\ \mathcal{L}_h(x, x + h_1\, e_1) & = 0 \text{ (set artificially to 0)}\,, \\ \mathcal{L}_h(x, x - h_1\, e_1) & = \dfrac{|f_1(x)|}{h_1} + \dfrac{\sigma_1^2(x)}{h_1^2}\,, \\ \mathcal{L}_h(x, x \pm h_2\, e_2) & = 0 \text{ because } f_2(s_{\max}, 0) = \sigma_2(s_{\max}, 0) = 0\,, \\ \mathcal{L}_h(x, y) & = 0 \qquad \text{otherwise.} \end{cases}$$

- For $x = (0, b_{\max})$

$$\begin{cases} \mathcal{L}_h(x,x) & = -\dfrac{|f_1(x)|}{h_1} - \dfrac{|f_2(x)|}{h_2} - \dfrac{\sigma_2^2(x)}{h_2^2}\,, \\ \mathcal{L}_h(x,x+h_1\,e_1) & = \dfrac{f_1^+(x)}{h_1}\,, \\ \mathcal{L}_h(x,x-h_1\,e_1) & = 0 \text{ because } f_1(0,b_{\max}) = D\,s_{\text{in}}\,, \quad \sigma_1(0,b_{\max}) = 0\,, \\ \mathcal{L}_h(x,x+h_2\,e_2) & = 0 \text{ (set artificially to 0)}\,, \\ \mathcal{L}_h(x,x-h_2\,e_2) & = \dfrac{|f_2(x)|}{h_2} + \dfrac{\sigma_2^2(x)}{h_2^2}\,, \\ \mathcal{L}_h(x,y) & = 0 \qquad \text{otherwise.} \end{cases}$$

- For $x = (s_{\max}, b_{\max})$

$$\begin{cases} \mathcal{L}_h(x,x) & = -\dfrac{|f_1(x)|}{h_1} - \dfrac{|f_2(x)|}{h_2} - \dfrac{\sigma_1^2(x)}{h_1^2} - \dfrac{\sigma_2^2(x)}{h_2^2}\,, \\ \mathcal{L}_h(x,x+h_1\,e_1) & = 0 \text{ (set artificially to 0)}\,, \\ \mathcal{L}_h(x,x-h_1\,e_1) & = \dfrac{|f_1(x)|}{h_1} + \dfrac{\sigma_1^2(x)}{h_1^2}\,, \\ \mathcal{L}_h(x,x+h_2\,e_2) & = 0 \text{ (set artificially to 0)}\,, \\ \mathcal{L}_h(x,x-h_2\,e_2) & = \dfrac{|f_2(x)|}{h_2} + \dfrac{\sigma_2^2(x)}{h_2^2}\,, \\ \mathcal{L}_h(x,y) & = 0 \qquad \text{otherwise.} \end{cases}$$

References

[1] H. Brézis, Functional Analysis, Sobolev Spaces and Partial Differential Equations, Springer, New York, Dordrecht, Heidelberg, London, 2010.
[2] F. Campillo, M. Joannides, I. Larramendy-Valverde, Stochastic modeling of the chemostat, Ecological Modelling 222 (2011) 2676–2689.
[3] J. Grasman, M. De Gee, Breakdown of a chemostat exposed to stochastic noise volume, Journal of Engineering Mathematics 53 (2005) 291–300.
[4] J. Grasman, O.A. van Herwaarden, Asymptotic Methods for the Fokker–Planck Equation and the Exit Problem in Applications, Springer-Verlag, Berlin, Heidelberg, 1999.
[5] N. Ikeda, S. Watanabe, Stochastic Differential Equations and Diffusion Processes, North-Holland/Kodansha, Amsterdam, 1981.
[6] L. Imhof, S. Walcher, Exclusion and persistence in deterministic and stochastic chemostat models, Journal of Differential Equations 217 (2005) 26–53.
[7] M. Joannides, I. Larramendy-Valverde, On geometry and scale of a stochastic chemostat, in: Stochastic Modeling Techniques and Data Analysis International Conference (SMTDA 2010), Chania, Crete, Greece, 2010.
[8] H.J. Kushner, Probability Methods for Approximations in Stochastic Control and for Elliptic Equations volume 129 of Mathematics in Science and Engineering, Academic Press, New York, 1977.
[9] H.J. Kushner, Numerical methods for stochastic control problems in continuous time, SIAM Journal on Control and Optimization 28 (1990) 999–1048.
[10] D. Lamberton, B. Lapeyre, Introduction to Stochastic Calculus Applied to Finance, Chapman & Hall/CRC, London, 1996.
[11] R. Lord, R. Koekkoek, D. van Dijk, A comparison of biased simulation schemes for stochastic volatility models, Quantitative Finance 10 (2010) 177–194.
[12] Z. Schuss, Theory and Applications of Stochastic Processes. An Analytical Approach, Springer, New York, Dordrecht, Heidelberg, London, 2010.
[13] H.L. Smith, P.E. Waltman, The Theory of the Chemostat: Dynamics of Microbial Competition, Cambridge University Press, New York, 1995.